

DEPARTMENT OF MATHEMATICS

ALGORITHM:–Andy's

Lagrange-Galerkin Offers Really Immense
Time-steps and Higher-order Monotonicity.
The Multidimensional Monotone and Nearly
Conservative Lagrange-Galerkin Method

with C^1 Elements

by

A. Priestley

Numerical Analysis Report 1/92

UNIVERSITY OF READING

ALGORITHM:–Andy’s
Lagrange-Galerkin Offers Really Immense
Time-steps and Higher-order Monotonicity.
The Multidimensional Monotone and Nearly
Conservative Lagrange-Galerkin Method
with C^1 Elements*

A. Priestley

Institute of Computational Fluid Dynamics,

Dept. of Mathematics,

University of Reading,

Whiteknights,

Reading,

U.K..

*The work reported here forms part of the research programme of the Reading/Oxford Institute for Computational Fluid Dynamics and was funded by the SERC.

0 Abstract

In this paper we consider **PLAGIARISM**, a direct Lagrange-Galerkin method due to Priestley, and address certain problems with both the Lagrange-Galerkin & **PLAGIARISM** methods which disappear with the use of higher-order C^1 basis functions. Here we concentrate on the use of Hermite-cubics, demonstrating their superior stability in the Lagrange-Galerkin method, and the adaptations of the **PLAGIARISM** technique needed to ensure monotonicity and near conservation.

AMS (MOS) Subject Classification Numbers:- 65M25, 65N30

Keywords:- Finite Elements, monotonicity, Euler equations, method of characteristics, Lagrange-Galerkin

Suggested Running Head:- Monotone Lagrange-Galerkin method with C^1 Elements

1 Introduction

In recent years the combination of the method of characteristics with the finite element method has proved quite popular, see Benqué et al [1], Bercovier & Pironneau [2], Douglas & Russell [11], Lesaint [20], Russell [32], Süli [38] and Pironneau [26], for example. The resulting Lagrange-Galerkin method has many desirable properties, often including unconditional stability, when the integrals can be performed exactly. Unfortunately this is rarely so and the introduction of quadrature reduces unconditional stability to unconditional instability in some cases, see Priestley [27] or Morton et al [25]. Moreover, the Lagrange-Galerkin method is not monotone, even with exact integration, and once inexact integration is used it is no longer conservative.

In Priestley [28] an adaptation of the Lagrange-Galerkin method is given that uses post-processing recovery operators in order to take the solution generated by the Lagrange-Galerkin method and recover a monotone and nearly conservative solution. This enables the Lagrange-Galerkin method to be applied to a much wider range of problems than has traditionally been the case. It also helps to nullify the stability problems raised by the use of quadrature. In this paper we suggest the use of a C^1 element to overcome problems with the slow convergence of the quadrature-based scheme to the exactly integrated method. We would also expect it to have a beneficial effect upon the stability of the scheme using inexact integration, c.f. [25]. First we describe the method.

Consider the Cauchy problem for the scalar linear advection equa-

tion for $u(\underline{x}, t)$:

$$(1.1) \quad u_t + \underline{a} \cdot \nabla u = 0, \quad \underline{x} \in \mathbb{R}^d, \quad t > 0,$$

$$(1.2) \quad u(\underline{x}, 0) = u_0(\underline{x}),$$

where u_0 belongs to $L^2(\mathbb{R}^d)$, d being the number of spatial dimensions. We can define characteristics paths or trajectories, $\underline{X}(\underline{x}, s; t)$, in two ways, either as the solution to an ordinary differential equation,

$$(1.3) \quad \underline{X}(\underline{x}, s; s) = \underline{x},$$

$$(1.4) \quad \frac{d\underline{X}(\underline{x}, s; t)}{dt} = \underline{a}(\underline{X}(\underline{x}, s; t), t);$$

or, if desired, as the solution of the integral equation

$$\underline{X}(\underline{x}, s; t) = \underline{x} + \int_s^t \underline{a}(\underline{X}(\underline{x}, s; \tau), \tau) d\tau.$$

In order to simplify the notation, for two time-levels t^n and $t^{n+1} = t^n + \Delta t$, we will denote the foot of the characteristic path at time t^n by \underline{x} and its arrival point at time t^{n+1} by \underline{y} . In terms of the notation in eqs. (1.3) and (1.4), these satisfy

$$\underline{x} = \underline{X}(\underline{y}, t^{n+1}; t^n) \quad \text{and} \quad \underline{y} = \underline{X}(\underline{x}, t^n; t^{n+1}).$$

A unique (absolutely continuous) solution to equations (1.3) and (1.4) can be guaranteed if it is assumed that \underline{a} belongs to the Bochner space

$L^1(0, T; (W^{1, \infty})^d)$, see Mizohata [23] for example. The solution to the original partial differential equation problem (1.1), (1.2) is now given by the relation

$$(1.5) \quad u(\underline{X}(\cdot, t, t + \tau), t + \tau) = u(\cdot, t), \quad t \geq 0, \tau \geq 0.$$

The direct Lagrange-Galerkin method, so called by Morton & Priestley [24], uses (1.5) directly to obtain a solution. For an approximation, U^n , at time t^n given in terms of finite element basis functions ϕ_j by

$$(1.6) \quad U^n(\cdot) = \sum_j U_j^n \phi_j(\cdot),$$

the direct Lagrange-Galerkin method uses eq. (1.5) to obtain U^{n+1} in $L^2(\mathbb{R}^d)$ at time t^{n+1} from the weak form of (1.5),

$$(1.7) \quad \langle U^{n+1}, \phi_i \rangle = \int U^n(\underline{x}) \phi_i(\underline{y}) d\underline{y} \quad \forall i,$$

i.e., from multiplying (1.5), with $t = t^n$ and $t + \tau = t^{n+1}$, by $\phi_i(\underline{y})$ and integrating over the whole domain with respect to \underline{y} , and the L^2 inner product over \mathbb{R}^d being denoted by $\langle \cdot, \cdot \rangle$. This is the same approach as that used by Bercovier & Pironneau [2], Douglas & Russell [11], Lesaint [20], Russell [32], Süli [38] and Pironneau [26], for example.

An alternative version of the method, due to Benqué et al [1], and termed the weak Lagrange-Galerkin method is more suited to equations in the conservation form

$$u_t + \underline{\nabla} \cdot (\underline{a}u) = 0.$$

A comparison of the two versions can be found in Priestley [27], Morton & Priestley [24] or Morton et al [25]. Due to the observations made in Priestley [28], i.e. the difficulty in constructing a low-order monotone scheme from the weak Lagrange-Galerkin method, only the direct Lagrange-Galerkin method will be considered here.

In Priestley [27] and Morton et al [25] it was shown that with linear elements the Lagrange-Galerkin scheme could become unstable when quadrature was used to approximate the integrals in (1.7). This analysis was later extended to include problems with diffusion by Süli [39]. In common with most finite element methods, the Lagrange-Galerkin method will generate oscillations at discontinuities: moreover the direct Lagrange-Galerkin method is not conservative. The weak Lagrange-Galerkin method will be conservative only if the mass matrix is inverted exactly and hence, in practice, this method is not quite conservative either.

In Priestley [28] a monotone version of the direct Lagrange-Galerkin method, called **PLAGIARISM**, was described. This deals with the problem of oscillations at discontinuities and also stops the scheme from blowing up because of the instabilities. Monotonicity was obtained by noting that if the mass matrix was lumped in the direct Lagrange-Galerkin method then it could be shown that the resulting scheme was monotone, albeit of very low accuracy. Given this low order, but monotone, scheme it is then possible to combine it with the high-order scheme obtained from inverting the full mass matrix to obtain a scheme that is

both accurate and monotone. This is the FCT (Flux-Corrected Transport) approach of Boris & Book [5] and Zalesak [46]. For an impressive example of the FCT algorithm applied to another finite element procedure see Löhner et al [21] for example.

Given the high-order solution U^H and the low-order solution U^L at a point i , we calculate the maximum value of α_i , $0 \leq \alpha_i \leq 1$, as in [28], such that the high-order monotone solution

$$U_i^M = \alpha_i U_i^H + (1 - \alpha_i) U_i^L$$

is bounded by values obtained from the solution at the previous time-level and values predicted by the monotone scheme.

In Priestley [28] a further modification was then applied that generally took these α values to be the maximum allowable but would then choose sub-optimal values in order to achieve conservation of U^M . This algorithm is fully described in [28]. Although conservation cannot be formally guaranteed at every time-step it was found that usually conservation was achieved to machine precision with no discernible loss of accuracy. The results obtained on the simple problem of advecting a square wave with a constant velocity showed the **PLAGIARISM** method to be only marginally worse than the TVD scheme using the Superbee limiter, see Roe [30], but substantially better than the TVD scheme using Van Leer's limiter, see Van Leer [42], the latter being generally regarded as the best of the rest of the limiters. Although the method did not perform quite as

well as Superbee it must be remembered that **PLAGIARISM**, unlike Superbee, has no CFL limit and can be readily extended to multi-dimensions.

The accuracy of the scheme was demonstrated for the exactly integrated version of the direct Lagrange-Galerkin method. Apart from the simple case used as a test problem in [28], quadrature must generally be used. Although the **PLAGIARISM** method reduces the stability problems associated with this aspect of the method there is still a problem with the convergence of the quadrature, i.e. with the convergence of the scheme using quadrature to that with exact integration. A test problem is that of constant coefficient linear advection in one-dimension on the domain $[0, 1]$ with periodic boundary conditions, that is,

$$u_t + u_x = 0$$

$$u(0) = u(1).$$

The initial data is chosen to be a square wave

$$u_0(x) = \begin{cases} 1 & 0.4 \leq x \leq 0.6 \\ 0 & \text{otherwise,} \end{cases}$$

as shown in figure (1). The Lagrange-Galerkin method can solve this problem rather well in just one time-step as there is no CFL stability limit, and so the CFL number was artificially restricted to take a value $1/12$ so that we can observe the accuracy after a large number of time-steps. The problem was run for

10 periods or revolutions. In figure (2) the solution is shown as calculated by the monotone direct Lagrange-Galerkin method, using exact integration and various Gauss-Lobatto quadratures. We can see that both the 3 pt. and 4 pt. quadrature rules offer very poor accuracy. The 5 pt. quadrature does rather better but still falls significantly short of the exactly integrated version. The schemes using 6 & 7 pt. quadrature fail because of stability problems. One of these is plotted to show the phase error incurred. Indeed it is not until 8 quadrature points are used that the approximately integrated version of **PLAGIARISM** overlaps the exactly integrated version of the method. Whilst 8 abscissae per element is reasonable for a one-dimensional calculation, the implication for two and three-dimensional problems is frightening. With this number of quadrature points the scheme is no more efficient than the EPIC algorithm of Eastwood & Arter [12], which uses a compound trapezium rule on each element to evaluate the integral on the right-hand side of eq. (1.7) and the mass matrix resulting from the integral on the left-hand side of (1.7). The EPIC algorithm has the added advantage of retaining the unconditional stability of the exactly integrated scheme. In Morton et al [25] it was claimed that the EPIC algorithm was inefficient compared to using the method with the exact mass matrix and a Gaussian quadrature to evaluate the right-hand sides. This is not the contradiction that it first appears. In [25] the authors were concerned with the advection of a much smoother profile, a Gaussian hill for example. With this data the integrals on the right-hand side can be evaluated very accurately with 4 or even 2 Gauss-Legendre points. On the other hand the EPIC algorithm has a partially lumped mass matrix because of the compound trapezium rule employed in the evaluation of these integrals and

hence still requires more points to be used to avoid significant diffusion being added to the problem.

In the following section the reason for the lack of convergence of the approximate integration in the **PLAGIARISM** algorithm is given together with a solution to the problem which involves the use of higher-order elements. These new elements will be partially analysed for their stability under quadrature. In section 3 the test problem given above and used in [28] will be run again with the new elements and be shown to give very accurate answers even with the use of quadrature. As a further demonstration of the possible applications of this method to non-traditional examples, a shock tube problem in gas dynamics is also solved, with no restrictions put on the scheme that would prevent its use in higher dimensions on arbitrary grids.

2 The Lagrange-Galerkin Method with C^1 Elements

2.1 Advantages of using C^1 Elements

C^0 elements, be they piecewise constants, piecewise linears or piecewise quadratics, are by far the most common elements used in CFD, in particular with the Lagrange-Galerkin method. The finite difference version of the Lagrange-Galerkin method, called the semi-Lagrangian method (see Staniforth & Côté [36] for a review of this method) has used cubic spline and Hermite-cubic interpolation. The

relationship between the two methods has been explored by Bermejo [3, 4]. Globally C^0 elements give a function that is continuous but has discontinuous first derivative. Whilst it may be an obvious statement it is still a rather important one that within each element these C^0 basis functions are actually C^∞ functions. This is significant because the integrals that arise from the finite element method are evaluated in an element-wise fashion. Generally this means that for most finite element methods the integrand is a C^∞ function over each sub-domain of integration. This smoothness of the integrand over the area of integration has consequences for the success of numerical integration.

Unfortunately, in the Lagrange-Galerkin method, eq. (1.7), the test functions are shifted upwind. Although the product of two linear basis functions, say, is still quadratic, it is now only piecewise quadratic within the element in question. Instead, then, of having an integrand that is a C^∞ function over each sub-domain of integration we have a function that is only C^0 on the element, the first derivative being discontinuous. Errors for quadrature formulae, see Demidovich & Maron [10] for example, approximating the integral

$$(2.1) \quad \int_a^b f(x) dx$$

by a Gauss-Legendre rule, are usually given in the form

$$(2.2) \quad R_n = \frac{(b-a)^{2n+1} (n!)^4 f^{(2n)}(\eta)}{[(2n)!]^3 (2n+1)},$$

where n is the number of abscissae and η is an unknown point in the range $a \leq \eta \leq b$. This implies that the quadrature converges to (2.1) like $O(1/(2n)!)$

which is faster than any power of n , but the problem with a formulae like (2.2) is the fact that $2n$ derivatives of the integrand are needed in order to apply it. Even the simple formulae for the remainder term with the compound trapezium rule,

$$R_n = -\frac{(b-a)^3}{12n^2} f^{(2)}(\eta)$$

requires the existence of two continuous derivatives. More sophisticated results are available, see Davis & Rabinowitz [8] for example, that do not rely on large numbers of derivatives existing. These results depend upon the theorems of Jackson [18] regarding the approximation of functions, with a given number of derivatives, by polynomials.

More generally, then, the error in approximating the integral (2.1), with a quadrature formula using only positive weights, is given by

$$E(f) = 2(b-a)\epsilon$$

where $\epsilon = \max |f(x) - p_n(x)|$, $x \in [a, b]$, is an estimate of how close a function of given continuity may be approximated by a polynomial, $p_n(x)$, of degree n or less. (If negative weights are allowed then the formula is given by $E(f) = \epsilon((b-a) + \sum_k |w_k|)$). Following Davis & Rabinowitz [8], we assume that if $f \in C^p$ then it has a bounded $(p+1)^{th}$ derivative, i.e.,

$$\|f\|_{p+1, \infty} = M_{p+1} \quad \text{for } f \in C^p.$$

Then, for $f \in C^0$ and $x \in [a, b]$,

$$(2.3) \quad |f(x) - p_n(x)| \leq \frac{3(b-a)M_1}{n}.$$

For $f \in C^p, p > 1$, we have the estimate

$$(2.4) \quad |f(x) - p_n(x)| \leq \frac{6^{p+1} p^p}{p! n^{p+1}} (p+1)(b-a)^{p+1} M_{p+1}.$$

Equation (2.3) is the reason for the slow convergence of the quadrature reported earlier. When the integrand in eq. (1.7) has discontinuous first derivative the quadrature will only converge linearly, no matter what the rule. There is still an advantage in using the Gaussian methods though. The n in eqs. (2.3) and (2.4) refers to the degree of polynomial being approximated, and hence for a k point quadrature we have for the compound trapezium rule $n = k - 1$ (which comes from the sub-division of $[a, b]$ rather than the degree of the polynomial) whilst for Gauss-Legendre quadrature we have $n = 2k - 1$ and for Gauss-Lobatto quadrature $n = 2k - 3$.

By using C^1 elements, the integrand in eq. (1.7) has continuous first derivative and discontinuous second derivative. Putting $p = 1$ into eq. (2.4) we see that quadratic convergence will now be obtained for the quadratures. Clearly this is quite a comedown from $O(1/(2n)!)$ convergence but as we shall see later it is sufficient for an efficient and accurate scheme to be obtained using quadrature.

Apart from accuracy considerations there may well be other advantages in using smoother basis functions. Süli & Ware [40] have taken the smooth-

ness of the basis functions to the extreme by using spectral methods. This means that the right-hand side of (1.7) remains infinitely smooth and they were able to prove the unconditional stability of the scheme even when using approximate integration. We may therefore hope that C^1 elements will exhibit better stability properties than their C^0 counterparts when quadrature is applied, see Morton et al [25].

The element we are going to use here is the Hermite-cubic. From the above discussion it may seem sensible to use the B-spline element because this is a C^2 element and hence has one more degree of continuity than the C^1 Hermite-cubic element. However, the B-spline element has a large support and this produces difficulties, though not insurmountable ones, at the boundaries, see Strang & Fix [37]. More important is the fact that the Hermite-cubic elements extend to triangular grids. The obvious extension is to construct the triangular element that has u, u_x & u_y as unknowns at the vertices together with u at the centroid to give the correct number of unknowns. This is labelled the Z_3 element in Strang & Fix [37] although there are more attractive versions of the same element, see Zienkiewicz [48], which may be more robust. Although this Z_3 element has some continuity of derivatives it is not a C^1 element. It is hoped, at a later date, to carry out numerical experiments to see whether there is enough continuity in this element to produce an efficient scheme with quadrature. Strictly C^1 triangular elements can be constructed in a number of ways, see [37]. Also see Mitchell & Wait [22] and Zienkiewicz [47].

Denoting the two variables at the node i , at time-level n , as the function value U_i^n and the derivative value $U_i'^n$, we can write down the value of the finite element approximation to the solution $u(x, t^n)$ in the element $[x_i, x_{i+1}]$ as

$$U^n(x) = U_i^n + U_i'^n x + (3U_{i+1}^n - 3U_i^n - U_{i+1}'^n h - 2U_i'^n h) \frac{x^2}{h^2} \\ + (2U_i^n - 2U_{i+1}^n + hU_{i+1}'^n + hU_i'^n) \frac{x^3}{h^3},$$

where $h = x_{i+1} - x_i$. Alternatively we can expand $U^n(x)$ on the element in terms of the element basis functions,

$$U^n(x) = U_i^n \phi_i \left(\frac{x}{h} \right) + U_i'^n \omega_i \left(\frac{x}{h} \right) + U_{i+1}^n \phi_{i+1} \left(\frac{x}{h} \right) + U_{i+1}'^n \omega_{i+1} \left(\frac{x}{h} \right),$$

where

$$(2.5) \quad \phi_i(z) = 2z^3 - 3z^2 + 1$$

$$(2.6) \quad \phi_{i+1}(z) = -2z^3 + 3z^2$$

$$(2.7) \quad \omega_i(z) = h(z^3 - 2z^2 + z)$$

$$(2.8) \quad \omega_{i+1}(z) = h(z^3 - z^2).$$

Now that we have two different types of basis functions, $\phi_i(x)$ and $\omega_i(x)$, the direct Lagrange-Galerkin method, eq. (1.7), is slightly modified in that there are

now a pair of equations,

$$(2.9) \quad \langle U^{n+1}, \phi_i \rangle = \int U^n(x) \phi_i(y) dy \quad \forall i,$$

and

$$(2.10) \quad \langle U^{n+1}, \omega_i \rangle = \int U^n(x) \omega_i(y) dy \quad \forall i.$$

At first sight it might seem that we now have twice the work per element that we would have had had we just chosen a cubic C^0 element and not the C^1 Hermite-cubic element. However, this is not the case. In the Lagrange-Galerkin method the predominant cost is the evaluation of the right-hand side integrals. This is due to the calculation of the trajectory from each quadrature point and then the interpolation of U^n at the foot of the trajectory. This only needs to be done once for equations (2.9) and (2.10), the two integrands differing only in that this interpolated value is then multiplied by two different cubics.

The only other issue is the efficiency with which the resulting linear equations can be solved. Wathen [43] showed that the conjugate gradient method, see Golub & Van Loan [14] for example, with diagonal preconditioning is a very efficient means of inverting the mass matrix arising from several common types of elements. With the usual element numbering, that is, $\dots U_i, U'_i, U_{i+1}, U'_{i+1} \dots$ the element mass matrix, M_E , with Hermite-cubic elements is given by

$$(2.11) \quad M_E = \frac{h}{420} \begin{pmatrix} 156 & 22h & 54 & -13h \\ 22h & 4h^2 & 13h & -3h^2 \\ 54 & 13h & 156 & -22h \\ -13h & -3h^2 & -22h & 4h^2 \end{pmatrix}.$$

With no preconditioning the condition number, κ , of the element mass matrix (putting $h = 1/100$ into eq. (2.11) for example) is $\kappa \approx 1.0 \times 10^7$. Premultiplying (2.11) by D^{-1} , where $D = \text{diag}(M_E)$, reduces the condition number to $\kappa \approx 76$ independently of the value of h . Following Wathen [44], this can be improved on yet further. Indeed the result for one-dimensional Hermite-cubic elements is a simpler example than the one presented in [44]. This involves preconditioning with the inverse of the block diagonal matrix B_D , given by,

$$B_D = \frac{h}{420} \begin{pmatrix} 156 & 22h & 0 & 0 \\ 22h & 4h^2 & 0 & 0 \\ 0 & 0 & 156 & -22h \\ 0 & 0 & -22h & 4h^2 \end{pmatrix},$$

which then leads to a very acceptable condition number of $\kappa \approx 13$.

We can now conclude that there is no reason not to use Hermite-cubic elements from the efficiency point of view. Compared to the more usual C^0 polynomial elements it is only marginally more expensive to calculate the integrands in the right-hand sides and again only slightly more expensive to solve

the system of linear equations that results.

2.2 Theoretical Results with Exact Integration

Although the main thrust of this paper is to describe the advantages of using C^1 elements in the direct Lagrange-Galerkin method when inexact integration has to be used, here we momentarily look at the theoretical results that can be obtained when exact integration is used. These are just extensions of the results given in Morton et al [25].

Let the velocity field $\underline{a}(\underline{x}, t)$ is assumed to be incompressible, i.e.

$$(2.12) \quad \nabla \cdot \underline{a} = 0 \quad \forall \underline{x}, t.$$

If J is the Jacobi matrix of the transformation defined by the mapping $\underline{X}(\cdot, t^n; t^{n+1})$, then we now have, as shown in Chorin & Marsden [6],

$$\frac{d|J|}{dt} = (\nabla \cdot \underline{a})|J|,$$

where $|J|$ is the determinant of J . For an incompressible velocity field, eq. (2.12) implies that

$$(2.13) \quad |J| = \text{constant} = 1,$$

which in turn implies that $d\underline{x} \equiv d\underline{y}$. Suppose now that we denote by $E_{\Delta t}(t)$ the solution operator $u(\cdot, t + \Delta t) = E_{\Delta t}(t)u(\cdot, t)$, and similarly $E_{\Delta t}^{-1}(t)u(\cdot, t + \Delta t) = u(\cdot, t)$, for equation (1.1) over the time-step Δt ; that is from (1.5)

$$(2.14) \quad E_{\Delta t}(t)u(\cdot, t) = u(\cdot, t + \Delta t) = u(\underline{X}(\cdot, t + \Delta t; t), t).$$

Letting $\| \cdot \|$ denote the usual L^2 norm over \mathbb{R}^d and $\| \cdot \|_*$ be the correspondingly defined operator norm, we have

$$\| E_{\Delta t}(t) \|_* = \sup_{u \neq 0} \frac{\| E_{\Delta t}(t)u(\cdot, t) \|}{\| u(\cdot, t) \|} = \sup_{u \neq 0} \frac{\| u(\cdot, t + \Delta t) \|}{\| u(\cdot, t) \|},$$

and from (2.14) and (2.13) this equals 1. Hence

$$(2.15) \quad \| E_{\Delta t}(t) \|_* = 1 = \| E_{\Delta t}^{-1}(t) \|_*.$$

The unconditional stability of the direct Lagrange-Galerkin method with Hermite-cubic basis functions now follows immediately. Rewriting equations (2.9) and (2.10) we have,

$$(2.16) \quad \langle U^{n+1}, \phi_i \rangle = \langle E_{\Delta t}(t)U^n, \phi_i \rangle$$

$$(2.17) \quad \langle U^{n+1}, \omega_i \rangle = \langle E_{\Delta t}(t)U^n, \omega_i \rangle.$$

Multiplying eq. (2.16) by U_i^{n+1} and eq. (2.17) by U_i^{n+1} and summing both equations over i and then summing the result gives

$$\begin{aligned} \| U^{n+1} \|^2 &= \langle U^n, E_{\Delta t}(t^n)U^{n+1} \rangle \\ &\leq \| E_{\Delta t}(t^n)U^n \| \cdot \| U^{n+1} \|. \end{aligned}$$

Using (2.15) and the Cauchy-Schwarz inequality, we have,

$$\| U^{n+1} \| \leq \| U^n \| .$$

Clearly this result does not depend on there just being the two types of basis functions, ϕ and ω , or indeed there being the same number at each node. As long as the function $U(\underline{x})$ can be written in the form

$$U(\underline{x}) = \sum_{i=\text{nodes}} \left(\sum_{k=\text{element types}} U_i^k \psi_i^k(\underline{x}) \right),$$

where $\psi_i^k(\underline{x})$ are the various element types being used, ϕ_i and ω_i in the case of the Hermite-cubics used here, then the same stability result can be proved. This means that the results also hold true for the Z_3 element and other two-dimensional elements.

As for convergence we have the following theorem.

THEOREM 1 *The direct Lagrange-Galerkin method with C^p finite elements of degree k ($k \geq p + 1$) converges with order $k - s$ in the $l^\infty(0, T; (L^{s,2})^d)$ norm, $0 \leq s \leq p + 1$, provided that $u_0 \in (H^{k+1})^d$, $\underline{a} \in L^\infty(0, T; (W^{1,\infty})^d)$ and the corresponding solution u of (1.1) belongs to the space $H^1(0, T; (H^{k+1})^d)$. The mesh is assumed to be quasi-uniform, i.e., $h_{\max}/h_k < C$ for every mesh length h_k .*

Proof

C will be taken to denote a generic constant.

Let $\eta^n = u^n - Iu^n$ and $\xi^n = Iu^n - U^n$, where u^n denotes the value of the solution

to equation (1.1) at time $t^n = n\Delta t$ and Iu^n is a piecewise polynomial interpolant of u^n of degree k . From (2.9) we have

$$\begin{aligned}
\langle \xi^{n+1} - E_{\Delta t}(t^n)\xi^n, \xi^{n+1} \rangle &= \langle Iu^{n+1} - E_{\Delta t}(t^n)Iu^n, \xi^{n+1} \rangle \\
&= \langle E_{\Delta t}(t^n)\eta^n - \eta^{n+1}, \xi^{n+1} \rangle \\
&= \langle E_{\Delta t}(t^n)\eta^n - \eta^n, \xi^{n+1} \rangle + \langle \eta^n - \eta^{n+1}, \xi^{n+1} \rangle.
\end{aligned}$$

Using (2.15) and applying the Cauchy-Schwarz inequality to all of the inner products we get

$$(2.18) \quad \|\xi^{n+1}\| \leq \|\xi^n\| + \|E_{\Delta t}(t^n)\eta^n - \eta^n\| + \|\eta^n - \eta^{n+1}\|.$$

It now remains to estimate the right-hand side terms in (2.18). Following the convergence proof in Süli [38],

$$\|E_{\Delta t}(t^n)\eta^n - \eta^n\| \leq C\Delta t \|\nabla\eta^n\|,$$

$$\|\eta^n - \eta^{n+1}\| \leq \int_{t^n}^{t^{n+1}} \left\| \frac{d\eta}{dt}(t) \right\| dt,$$

so that

$$\|\xi^n\| \leq \|\xi^0\| + \left\| \frac{d\eta}{dt} \right\|_{L^1(0,T;(L^2)^d)} + C \|\nabla\eta\|_{L^\infty(0,T;(L^2)^d)}.$$

Assuming that U^0 has been chosen to be Iu^0 , standard interpolation results yield the desired estimate:

$$(2.19) \quad \|u - U\|_{l^\infty(0,T;(L^2)^d)} \leq Ch^k \|u\|_{H^1(0,T;(H^{k+1})^d)}.$$

For the estimates on the derivative errors we write,

$$(2.20) \quad \begin{aligned} \|u - U\|_{l^\infty(0,T;(H^s)^d)} &\leq \|u - Iu\|_{l^\infty(0,T;(H^s)^d)} + \|Iu - U\|_{l^\infty(0,T;(H^s)^d)} \\ &\leq Ch^{k-s} \|u\|_{l^\infty(0,T;(H^k)^d)} + \|Iu - U\|_{l^\infty(0,T;(H^s)^d)}. \end{aligned}$$

It now remains to bound $\|Iu - U\|_{l^\infty(0,T;(H^s)^d)}$. Using Ciarlet [7] (Theorem 3.2.6),

$$\begin{aligned} \|Iu - U\|_{l^\infty(0,T;(H^s)^d)} &\leq Ch^{-s} \|Iu - U\|_{l^\infty(0,T;(L^2)^d)} \\ &\leq Ch^{-s} \left(\|Iu - u\|_{l^\infty(0,T;(L^2)^d)} + \|u - U\|_{l^\infty(0,T;(L^2)^d)} \right), \end{aligned}$$

which, when using standard interpolation results and (2.19) becomes

$$(2.21) \quad \leq Ch^{-s} \left(h^k \|u\|_{l^\infty(0,T;(H^k)^d)} + h^k \|u\|_{H^1(0,T;(H^{k+1})^d)} \right).$$

Finally, combining (2.20) and (2.21) we have,

$$\|u - U\|_{l^\infty(0,T;(H^s)^d)} \leq Ch^{k-s} \|u\|_{H^1(0,T;(H^{k+1})^d)}$$

and hence

$$\|u - U\|_{l^\infty(0,T;(H^s)^d)} \leq Ch^{k-s} \|u\|_{H^1(0,T;(H^{k+1})^d)} \text{ for } 1 \leq s \leq p+1.$$

2.3 Stability and Inexact Integration

The unconditional stability of the exactly integrated method, just proved, is unfortunately not the end of the story. Priestley [27] and Morton et al [25] demonstrated that the Lagrange-Galerkin method with piecewise linear elements loses its stability properties when quadrature is applied, to leave a scheme unconditionally unstable or, at best, a scheme that is stable for only a very small range of CFL numbers. They considered a general quadrature on the interval $[0, 1]$ of the form,

$$(2.22) \quad \int_0^1 f(x)dx \approx w_0 f(0) + \sum_1^m w_k f(x_k) + w_{m+1} f(1),$$

where the weights w_0, \dots, w_{m+1} and the quadrature points $0 < x_1 < \dots < x_m < 1$ are free to be chosen, except that the quadrature was assumed to evaluate the integral of quadratic polynomials exactly. By considering CFL numbers, $\nu \in [0, x_1]$ they were able to show that the schemes were unstable. Negative results though are easy to prove, as the instability of the method only has to be demonstrated for one value of ν for the scheme to lose its unconditional stability. The Fourier analysis gets harder as the degree of the polynomial increases and yet more harder when two unknowns are present at each node. So far it has proved impossible to give any rigorous answer to the question of the scheme's stability when using quadrature. We can, however, go some way to demonstrating the superior stability of the method with Hermite-cubic elements over the method using C^0 elements.

A quadrature of the form used in (2.22) is taken except that now it

is assumed to integrate sextic polynomials. Considering the j^{th} pair of equations, we have

$$M \begin{pmatrix} U_j^{n+1} \\ U_j^{m+1} \end{pmatrix} = \begin{pmatrix} b_{j,1}^n \\ b_{j,2}^n \end{pmatrix},$$

where, with the usual notation of $\delta^2 U_j = (U_{j+1} - 2U_j + U_{j-1})$ and $\Delta_0 U_j = U_{j+1} - U_{j-1}$,

$$M = \begin{pmatrix} 1 + \frac{9\delta^2}{70} & -\frac{13h^2\Delta_0}{420} \\ \frac{13h^2\Delta_0}{420} & \frac{h^3}{420}(2 - 3\delta^2) \end{pmatrix}$$

and

$$\begin{aligned} b_{j,1}^n &= \left[\left(1 + \frac{9\delta^2}{70} \right) + \frac{42}{70}\nu^2\delta^2 + \nu^3\Delta_0 - \frac{\nu}{2}\Delta_0 + w_0(-2\nu^3\delta^2 - 3\nu^2\Delta_0) \right] U_j^n \\ &+ h \left[-2\nu^3 + \frac{\nu}{10}\delta^2 - \frac{13}{420}\Delta_0 - \frac{21}{420}\nu^2\Delta_0 + w_0(\nu^3\Delta_0 + \nu^2\delta^2 + 6\nu^2) \right] U_j^m \\ b_{j,2}^n &= \left[\frac{70}{420}\nu^3\delta^2 - \frac{42\nu}{420}\delta^2 + \frac{13}{420}\Delta_0 + \frac{21\nu^2}{420}\Delta_0 \right] U_j^n \\ &+ h \left[\frac{1}{420}(2 - 3\delta^2) + \frac{\nu^2}{60}(\delta^2 - 6) + \frac{\nu}{60}\Delta_0 - \frac{\nu^3}{12}\Delta_0 \right] U_j^m. \end{aligned}$$

We can now write the solution at the new time-level in terms of the solution at the old time-level multiplied by an amplification matrix, A ,

$$(2.23) \quad \begin{pmatrix} U_j^{n+1} \\ U_j^{m+1} \end{pmatrix} = A(\nu, \theta; w_0) \begin{pmatrix} U_j^n \\ U_j^m \end{pmatrix}.$$

The difference operators δ^2 and Δ_0 have been replaced by their Fourier expansions and hence the dependence on the Fourier angle θ in (2.23). The norm of the matrix A now determines the stability of the scheme. Denoting the two eigenvalues of A by λ_1 and λ_2 we can then define the 2 norm of A as

$$\| A \|_2 = \max(|\lambda_1|, |\lambda_2|).$$

It does not seem possible to make any analytic statements about this quantity. However, we can plot $\| A \|_2$ for any value of w_0 we choose and gain some insight into the stability of the scheme under a given quadrature. The lowest order Gaussian quadratures that satisfy the criterion that they integrate polynomials of degree 6 are the 4pt. Gauss-Legendre rule and the 5pt. Gauss-Lobatto rule. These have respective values of $w_0 = 0$ and $1/20$ and $x_1 = 0.0694$ and 0.17267 which are then bounds on the CFL number ν . In figure (3) there is a plot of a normalized value of $\| A \|_2$ and we see that everywhere $\| A \|_2 \leq 1$. Note also that because all higher order Gauss-Legendre quadratures still have $w_0 = 0$ and have $x_1 \leq 0.0694$ then this means that all Gauss-Legendre quadratures with 4 or more points are stable for $\nu \leq x_1$. A more convincing result is obtained for the 5pt. Gauss-Lobatto quadrature, because the value of x_1 is so much larger and hence a larger range of CFL numbers is covered. Figure (4) shows a plot of a normalized value of $\| A \|_2$ for this quadrature and again we see that $\| A \|_2 \leq 1$ and so we have stability. Conceivably this analysis could be repeated for $\nu \in [x_1, x_2]$ etc. but these results would be very specific to the quadrature used.

In conclusion then we can say that the stability is much improved over that of the C^0 linear element. We do not have unconditional stability though as the 4pt. Gauss-Legendre rule is unstable at $\nu = 5/12$. No instability has yet been observed with any other Gauss-Legendre or Gauss-Lobatto rule with 5 or more abscissae.

2.4 Monotonicity and Inexact Integration

In Priestley [28] it was proved that for linear elements the direct Lagrange-Galerkin method produces a monotone solution when the mass matrix is lumped. Although not explicitly stated there, this proof critically depended upon the fact that with piecewise linear finite elements the maximum value of the solution occurs at a node. For the Hermite-cubic element a slightly more sophisticated approach is needed, using eq. (2.9), however, in an entirely similar way to the proof in [28], where the basis functions $\phi_i(x)$ are now the monotone cubic functions given in (2.5) and (2.6). This enables us to make the following statements about the nodal values at the new time-level. If the solution at the previous time-level, U^n , was monotone between nodes, then

$$U_i^{n+1} \leq \max_j U_j^n \quad \forall i.$$

Alternatively, if the maximum occurs between nodes then we can still bound the new nodal values by

$$U_i^{n+1} \leq \max_x U^n(x) \quad \forall i.$$

Similar results can also be proved for the minimum. Indeed this second, more general result, opens up the possibility of applying sub-cell resolution ideas, c.f. Harten [15].

Unfortunately the fact that no new extrema can be generated at nodes does not prevent new extrema from being generated within the elements. This can occur because of the oscillatory nature of the basis functions, ω_i , associated with the derivative terms, eqs. (2.7) and (2.8). However, monotonicity within the element can be ensured by limiting the derivative values. This is a very simple procedure and is derived in Fritsch & Carlson [13]. It is also used in the monotone semi-Lagrangian method of Rasch & Williamson [29], Williamson & Rasch [45], which is a finite difference scheme with much in common with the direct Lagrange-Galerkin method with Hermite-cubic elements presented here. It is perhaps also worth comparing with the way in which the limiting is performed in the construction of the one-dimensional TVD (Total Variation Diminishing) schemes, see Sweby [41] for example.

Remark. Despite the fact that it is possible to make the scheme strictly monotone, in all the results presented in the next section it was found possible to obtain identical results just by limiting the function values without limiting the derivative values. This is not as pleasing theoretically but has important implications in applying the method in higher dimensions. Whilst the above result can be extended to elements on rectangles that are tensor products of the one-dimensional Hermite-cubic element, it is not at all clear how similar results

could be obtained for the Z_3 element or the quintic C^1 triangular elements and hence if it is unnecessary to limit the derivatives this would be very useful in the practical application of the method.

3 Test Problems and Results

The first test problem is that of constant linear advection in one dimension, the details being given in the introduction. The problem is run until $t = 10$, i.e., over 10 periods. To make this a worthwhile test for a Lagrangian scheme the time-step is restricted so that the effects of interpolation, approximate integration, and the projection error, may be allowed to accumulate.

Figure (5) compares the solution obtained by the Lagrange-Galerkin method with Hermite-cubic elements using a 5 point Gauss-Legendre quadrature to that obtained with the Superbee limiter. The number of nodes used for the Lagrange-Galerkin method was 50. The number of unknowns is hence 100 due to the use of the Hermite-cubic element. The cost, though, is by no means doubled because of the amount of shared work. The solution obtained by Superbee is shown with both 50 and 100 nodes. The l_2 error for the Lagrange-Galerkin method is 2.566×10^{-2} whereas for the two Superbee solutions it is 1.012×10^{-1} and 7.1×10^{-2} . The Lagrange-Galerkin solution is therefore more accurate in this norm. The solution obtained by the Lagrange-Galerkin method does under-shoot and overshoot though and hence, although formally more accurate, may not be such a desirable solution as that obtained by the Superbee limiter. The

other thing to note from this figure is the fact that such an accurate solution was obtained with a relatively low-order quadrature scheme. In figure (6) the monotone version of the Lagrange-Galerkin solution is plotted together with the non-monotone version and the Superbee solution on the same grid for reference. The l_2 error of this monotonised version increases, as we would expect, to 8.49×10^{-2} , which makes it now slightly less accurate than the Superbee limited solution with the same number of unknowns. Again we note that this has been achieved with a 5 point Gauss-Legendre quadrature whereas in Priestley [28] exact integration failed to get results as good. It is also worth noting again that although Superbee just beats the method here, the Lagrange-Galerkin method has no stability limit and is equally applicable in two-dimensions on quadrilateral or triangular elements.

The Lagrange-Galerkin method has traditionally just been used for the advective terms in fluid flow problems. In the Navier-Stokes equations, see Benqué et al [1] or Süli [38], the Lagrange-Galerkin method not only removes the CFL limit but then leaves a Stokes problem to be solved. A Stokes problem leads to a symmetric matrix which is then relatively easy to solve.

However, with the introduction of monotonicity and conservation the method can now be regarded as a general solver for any wave model. Conservation gives correct shock speeds, Lax & Wendroff [19], whilst monotonicity ensures convergence, Sanders [33]. Wave models are at the heart of most modern schemes for solving the Euler equations, see Roe [31], for example. These rely

upon the fact that disturbances to the solution can be expressed as the sum of a number of wave problems, three for the one-dimensional Euler equations, see Smoller [34] for details. In particular, then, the one-dimensional Euler equations in conservation form are given by,

$$(3.1) \quad \underline{u}_t + \underline{F}_x = \underline{0},$$

where

$$(3.2) \quad \underline{u} = \begin{pmatrix} \rho \\ m \\ e \end{pmatrix}, \quad \underline{F} = \begin{pmatrix} m \\ p + m^2/\rho \\ u(p + e) \end{pmatrix}.$$

In equation (3.2) ρ = density, u = velocity, $m = \rho u$ = momentum, p = static pressure and e is the total energy and is related to the other variables by an equation of state, which for a perfect gas is

$$e = \frac{p}{(\gamma - 1)} + \frac{1}{2}\rho u^2.$$

The constant γ is the ratio of specific heats and takes a value of 1.4 for our calculations. Two other variables that we shall need to define are the total enthalpy, $h = (e + p)/\rho$ and the sound speed, $a = (\gamma p/\rho)^{\frac{1}{2}}$. We define the Jacobian matrix to be $A = \partial \underline{F}/\partial \underline{u}$, where \underline{F} and \underline{u} are as in (3.2). The eigenvalues, λ , and right eigenvectors, \underline{e} , of A are then given by:-

$$\lambda_1 = u - a, \quad \lambda_2 = u \quad \text{and} \quad \lambda_3 = u + a,$$

$$\underline{e}_1 = \begin{pmatrix} 1 \\ u - a \\ h - ua \end{pmatrix}, \quad \underline{e}_2 = \begin{pmatrix} 1 \\ u \\ \frac{1}{2}u^2 \end{pmatrix} \quad \text{and} \quad \underline{e}_3 = \begin{pmatrix} 1 \\ u + a \\ h + ua \end{pmatrix}.$$

It now remains to find the strengths, α , of these waves such that

$$\underline{F}_x = \sum_{k=1}^3 \alpha_k \lambda_k \underline{e}_k.$$

The α_k can be shown to be,

$$\alpha_1 = \frac{\rho}{2a^2} [p_x - \rho a u_x], \quad \alpha_2 = \rho \left[\rho_x - \frac{1}{a^2} p_x \right] \quad \text{and} \quad \alpha_3 = \frac{\rho}{2a^2} [p_x + \rho a u_x].$$

The updates, $\alpha_k \lambda_k \underline{e}_k$, now satisfy the advection equation (1.1) with the velocity a now being replaced by each λ_k in turn. In solving these three advection problems and adding the updates to the previous solution we solve the original set of equations, (3.1) and (3.2). We have thus replaced the original equations with a set of wave problems for which the scheme presented here is suitable.

The test problem is that due to Sod [35]. This consists of two constant states on the domain $[0, 1]$ separated by a discontinuity at 0.5. The left-hand state is defined by $\rho_L = 1$, $p_L = 1$, $u_L = 0$, and the right-hand state by $\rho_R = 1/8$, $p_R = 1/10$, $u_R = 0.0$. The output time is $t = 0.144$. The results can be compared to those obtained by Sweby [41] for various TVD schemes using a variety of limiters.

There was one slight change to the monotone and nearly conservative algorithm of [28] which is also used here. The ‘low-order’ solution seems to have a tendency to develop nonphysical expansion shocks, so that an entropy condition is needed to ensure convergence to the correct physical solution, see Harten et al [16]. Whilst, at the moment, we have no theory to explain this or prove that the high-order solution will not also suffer from entropy violating solutions, the remedy is very simple. A small amount of artificial viscosity is added to the low-order solution. Where q represents an arbitrary quantity we just add the following quantity to the i^{th} node,

$$\epsilon \frac{\Delta t}{\Delta x^2} (q_{i+1}^{n+1} - 2q_i^{n+1} + q_{i-1}^{n+1}),$$

where a regular mesh spacing has been assumed. (At one point, in order to reduce the amount of diffusion especially across the contact discontinuity, this quantity was scaled by a factor $|p_{i,xx}| / \max_{j=nodes} |p_{j,xx}|$. Due to the small amounts eventually used this was probably an unnecessary complication.) A typical value of ϵ was 1.0×10^{-10} .

The first result, figure (7), is for the Lagrange-Galerkin method with the Hermite-cubic elements but without the monotonicity and conservation algorithms. These results are perhaps rather better than one might have expected, the basics of the solution all being there. There are a number of faults though. There is undershoot in front of the shock, most noticeable in the plot of velocity. This does appear, though, to be the only undershoot or overshoot in the entire solution. Rather more important is the error in the shock position, most

noticeable in the plots of pressure and density. The shock has clearly not travelled fast enough. This would seem to be due to the lack of conservation. For the conserved variables of (3.2) percentage conservations are $(99.25, 95.975, 98.79)^T$. In figure (8) we have applied the monotonicity and conservation algorithm, all other factors remaining the same. Conservation is now 100%, the undershoot has gone and more importantly the shock is now in the correct position. We believe, comparing with the results in Sweby [41], that these solutions are better than those from a TVD limiter scheme, with the exception of the Superbee limiter which captures the contact discontinuity slightly better, as we might expect from the results using linear advection. At the risk of repeating ourselves we stress again the flexibility of the scheme presented here as opposed to specialist one-dimensional nature of the Superbee scheme and the TVD methods in general.

Both these figures used a relatively high-order 8 point Gauss-Lobatto quadrature. In figure (9) we repeat the result of fig. (8) but using the 4 point Gauss-Legendre rule. There is no visible difference in an implementation costing about 50% of the previous result. This again demonstrates the improved convergence properties of the approximate integration when Hermite-cubic elements are used.

Although these tests on the Euler equations are at a very early stage they do appear to be very encouraging, giving results as good as the specialist one-dimensional TVD schemes. Given that this method can be applied, virtually unaltered, in two-dimensions on triangular or quadrilateral grids the

multi-dimensional wave models of the Euler equations due to Deconinck et al [9], Hirsch & Lacor [17] and Roe [31] would be an obvious further use of this method.

4 Conclusions

In this paper we have seen how the **PLAGIARISM** method of Priestley [28] can be extended to C^1 elements, namely Hermite-cubic elements. This improves the stability of the underlying direct Lagrange-Galerkin method and improves the effectiveness of the quadrature needed to evaluate the resulting integrals in all but the simplest problems. The algorithm has also been applied to the Euler equations showing how, with monotonicity and conservation, it can be used to solve more general wave problems.

References

- [1] Benqué, J.P., Labadie, G. & Ronat, J., “*A New Finite Element Method for the Navier-Stokes Equations Coupled with a Temperature Equation.*” Proc. 4th Int. Symp. on Finite Element Methods in Flow Problems (Ed. T. Kawai), North-Holland, Amsterdam, Oxford, New York, pp. 295-301, 1982.

- [2] Bercovier, M. & Pironneau, O., “*Characteristics and the Finite Element Method.*” Proc. 4th Int. Symp. on Finite Element Methods in Flow Problems (Ed. T. Kawai), North-Holland, Amsterdam, Oxford, New York, pp. 67-73, 1982.

- [3] Bermejo, R., “*On the Equivalence of semi-Lagrangian Schemes and Particle-in-Cell Finite Element Methods.*” Mon. Wea. Rev., **118**, pp. 979-987, 1990.

- [4] Bermejo, R., “*Analysis of an Algorithm for the Galerkin-characteristic Method.*” Numer. Math., **60**, pp. 163-194, 1991.

- [5] Boris, J.P. & Book, D.L., “*Flux Corrected Transport, I, SHASTA, A Fluid Transport Algorithm that Works.*” J. Comp. Phys., **11**, pp. 38-69, 1973.

- [6] Chorin, A.J. & Marsden, J.E., “*A Mathematical Introduction to Fluid Mechanics (Universitext).*” Springer-Verlag, New York, Berlin, Heidelberg,

Tokyo, 1984.

- [7] Ciarlet, P., "*The Finite Element Method for Elliptic Problems.*" North-Holland, Amsterdam, New York, Oxford, 1978.

- [8] Davis, P.J. & Rabinowitz, P., "*Methods of Numerical Integration.*" Academic Press, New York, London, 1975

- [9] Deconinck, H., Hirsch, Ch. & Peuteman, J., "*Characteristic Decomposition Methods for the Multidimensional Euler Equations.*" Lecture Notes in Physics **264**, pp. 216-221, Springer, 1986.

- [10] Demidovich, B.P. & Maron, I.A., "*Computational Mathematics.*" Mir Publishers, Moscow, 1987.

- [11] Douglas Jr., J. & Russell, T.F., "*Numerical Methods for Convection-Dominated Diffusion Problems based on combining the Method of Characteristics with Finite Element or Finite Difference Procedures.*" SIAM J. Numer. Anal., **19**, pp. 871-885, 1982.

- [12] Eastwood, J.W. & Arter, W., "*EPIC — Beyond the Ultimate Difference Scheme.*" Numerical Methods for Fluid Dynamics II, pp. 581-593, (Ed. K.W.

Morton & M.J. Baines), O.U.P., Oxford, 1986.

- [13] Fritsch, F.N. & Carlson, R.E., *Monotone Piecewise Cubic Interpolation.*"
SIAM J. Numer. Anal., **17**, pp. 238-246, 1980.

- [14] Golub, G.H. & Van Loan, C.F., "*Matrix Computations.*" Second Edition,
The John Hopkins University Press, Baltimore and London, 1989.

- [15] Harten, A., "*ENO Schemes with Subcell Resolution.*" CAM Report 87-13,
Dept. of Mathematics, University of California, Los Angeles, CA 90024-1555,
1987.

- [16] Harten, A., Hyman, J.M. & Lax, P.D., "*On Finite-Difference Approxima-
tions and Entropy Conditions for Shocks.*" Comm. Pure Appl. Maths., **29**,
pp. 297-322, 1976.

- [17] Hirsch, C. & Lacor, C., "*Upwind Algorithms based on a Diagonalization of
the Multidimensional Euler Equations.*" AIAA paper 89-1958, 1989.

- [18] Jackson, D., "*The Theory of Approximation.*" Amer. Maths. Soc. Colloquium
Publications, Vol. XI, New York, 1930.

- [19] Lax, P.D. & Wendroff, B., "*Systems of Conservation Laws.*" *Comm. Pure Appl. Maths.*, **13**, pp. 217-237, 1960.
- [20] Lesaint, P., "*Numerical Solution of the Equation of Continuity.*" *Topics in Numerical Analysis III* (Ed. J.J.H. Miller), Academic Press, London, New York, San Francisco, pp. 199-222, 1977.
- [21] Löhner, R., Morgan, K., Peraire, J. & Vahdati, M., "*Finite Element Flux-Corrected Transport (FEM-FCT) for the Euler and Navier-Stokes Equations.*" *Int. J. Numer. Meth. Fluids*, **7**, pp. 1093-1109, 1987.
- [22] Mitchell, A.R. & Wait, R., "*The Finite Element Method in Partial Differential Equations.*" John Wiley & Sons, Chichester & New York, 1977.
- [23] Mizohata, S., "*The Theory of Partial Differential Equations.*" Cambridge University Press, 1973.
- [24] Morton, K.W. & Priestley, A., "*On Characteristic and Lagrange-Galerkin Methods.*" *Pitman Research Notes in Mathematics Series* (Ed. D.F. Griffiths & G.A. Watson), Longman Scientific and Technical, Harlow, pp. 157-172, 1986.

- [25] Morton, K.W., Priestley, A. & Süli, E., “*Stability of the Lagrange-Galerkin Method with Non-Exact Integration.*” *RAIRO Modél. Math. Anal. Numér.*, **22**, no. 4, pp. 625-653, 1988.
- [26] Pironneau, O., “*On the Transport Diffusion Algorithm and its Application to the Navier-Stokes Equations.*” *Numer. Math.*, **38**, pp. 309-332, 1982.
- [27] Priestley, A., “*Lagrange and Characteristic Galerkin Methods for Evolutionary Problems.*” D.Phil. Thesis, Oxford University, 1986.
- [28] Priestley, A., “**PLAGIARISM:-***Priestley’s Lagrange-Galerkin Is A Really Interesting Scheme & Monotone. The Multidimensional Monotone and Nearly Conservative Lagrange-Galerkin Method.*” University of Reading Numerical Analysis Report 15/91, Dept. of Mathematics, University of Reading, Reading. Submitted to *IMA J. of Numer. Anal.*, 1992.
- [29] Rasch, P.J. & Williamson, D.L., “*On Shape-Preserving Interpolation and Semi-Lagrangian Transport.*” *SIAM J. Sci. Stat. Comput.*, **11**, pp. 656-687, 1990.
- [30] Roe, P.L., “*Large Scale Computations in Fluid Mechanics.*” *Lectures in Applied Mathematics*, **22**, no. 2, pp. 163-193, 1985.

- [31] Roe, P.L., "*Discrete Models for Numerical Analysis of Time-Dependent Multi-Dimensional Gas Dynamics.*" J. Comp. Phys, **63**, pp. 458-476, 1986.
- [32] Russell, T.F., "*Time Stepping along Characteristics with Incomplete Iteration for a Galerkin Approximation of Miscible Displacement in Porous Media.*" Ph.D. Thesis, University of Chicago, 1980.
- [33] Sanders, R., "*On Convergence of Monotone Finite Difference Schemes with Variable Spatial Differencing.*" Math. Comp., **40**, pp. 91-106, 1983.
- [34] Smoller, J., "*Shock Waves and Reaction-Diffusion Equations.*" Springer-Verlag, New York, 1983.
- [35] Sod, G.A., "*A Survey of Several Finite Difference Methods for Systems of Nonlinear Hyperbolic Conservation Laws.*" J. Comp. Phys., **27**, pp. 1-31, 1978.
- [36] Staniforth, A. & Côté, J., "*Semi-Lagrangian Integration Schemes for Atmospheric Models — A Review.*" Mon. Wea. Rev., **119**, pp. 2206-2223, 1991.

- [37] Strang, G. & Fix, G.J., "*An Analysis of the Finite Element Method.*" Prentice-Hall, New Jersey, 1973.
- [38] Süli, E., "*Convergence and Nonlinear Stability of the Lagrange-Galerkin Method for the Navier-Stokes Equations.*" Numer. Math., **53**, pp. 459-483, 1988.
- [39] Süli, E., "*Stability and Convergence of the Lagrange-Galerkin Method with Non-Exact Integration.*" The Mathematics of Finite Elements and Applications VI, MAFELAP 1987 (Ed. J.R. Whiteman), Academic Press, London, New York, San Francisco, pp. 435-442, 1988.
- [40] Süli, E. & Ware, A., "*A Spectral Method of Characteristics for Hyperbolic Problems.*" SIAM J. Numer. Anal., **28**, pp. 423-445, 1991.
- [41] Sweby, P.K., "*High Resolution Schemes Using Flux Limiters for Hyperbolic Conservation Laws.*" SIAM J. Numer. Anal., **21**, pp. 995-1011, 1984.
- [42] Van Leer, B., "*Towards the Ultimate Conservative Difference Scheme II. Monotonicity and Conservation Combined in a Second Order Scheme.*" J. Comp. Phys., **14**, pp. 361-371, 1974.

- [43] Wathen, A.J., "*Realistic Eigenvalue Bounds for the Galerkin Mass Matrix.*"
IMA J. Numer. Anal., **7**, pp. 449-457, 1987.
- [44] Wathen, A.J., "*Spectral Bounds and Preconditioning Methods using Element-by-Element Analysis for Galerkin Finite Element Equations.*" The Mathematics of Finite Elements and Applications VI, MAFELAP 1987 (Ed. J.R. Whiteman), Academic Press, London, New York, San Francisco, pp. 157-168, 1988.
- [45] Williamson, D.L. & Rasch, P.J., "*Two-Dimensional Semi-Lagrangian Transport with Shape-Preserving Interpolation.*" Mon. Wea. Rev., **117**, pp. 102-129, 1989.
- [46] Zalesak, S.T., "*Fully Multidimensional Flux-Corrected Transport Algorithms for Fluids.*" J. Comp. Phys., **31**, pp. 335-362, 1979.
- [47] Zienkiewicz, O.C., "*The Finite Element Method in Structural and Continuum Mechanics.*" McGraw-Hill, New York, 1967.
- [48] Zienkiewicz, O.C., "*The Finite Element Method in Engineering Science.*" McGraw-Hill, New York, 1971.

List of Figures

1	Initial data for advection problem.	43
2	Constant advection after ten rotations. Exact solution—solid line, Monotone 3,4,5,7 (with large phase error) & 8 pt. Gauss-Lobatto— \square 's, Monotone exact integration— \times . $\Delta x = 1/100$, $\nu = 1/12$	44
3	Plot of $(\ A\ _2 - 1) \times 10^6$ for Gauss-Legendre quadrature. Ranges of θ & ν are $[0, 2\pi] \times [0, 0.07]$. $\max(\ A\ _2) = 1$, $\min(\ A\ _2) = 0.999947$	45
4	Plot of $(\ A\ _2 - 1) \times 10^6$ for 5 point Gauss-Lobatto quadrature. Range of θ & ν are $[0, 2\pi] \times [0, 0.18]$. $\max(\ A\ _2) = 1$, $\min(\ A\ _2) = 0.998542$	46
5	Constant advection after ten rotations. Exact solution—solid line, Superbee ($\Delta x = 1/50$)—+, Superbee ($\Delta x = 1/100$)—*, Lagrange-Galerkin using 5pt. Gauss-Legendre quadrature— \times . $\nu = 5/12$	47
6	Constant advection after ten rotations. Exact solution—solid line, Superbee —+, Lagrange-Galerkin using 5pt. Gauss-Legendre quadrature— \times , monotone Lagrange-Galerkin using 5pt. Gauss-Legendre — Δ . $\nu = 5/12$, $\Delta x = 1/50$	48
7	Sod's problem with the Lagrange-Galerkin method evaluated by 8 pt. Gauss-Lobatto quadrature. $\max \nu = 0.22$, $\Delta x = 1/100$	49
8	Sod's problem with monotonic Lagrange-Galerkin evaluated by 8 pt. Gauss-Lobatto quadrature. $\max \nu = 0.22$, $\Delta x = 1/100$	50
9	Sod's problem with monotonic Lagrange-Galerkin evaluated by 4 pt. Gauss-Legendre quadrature. $\max \nu = 0.22$, $\Delta x = 1/100$	51

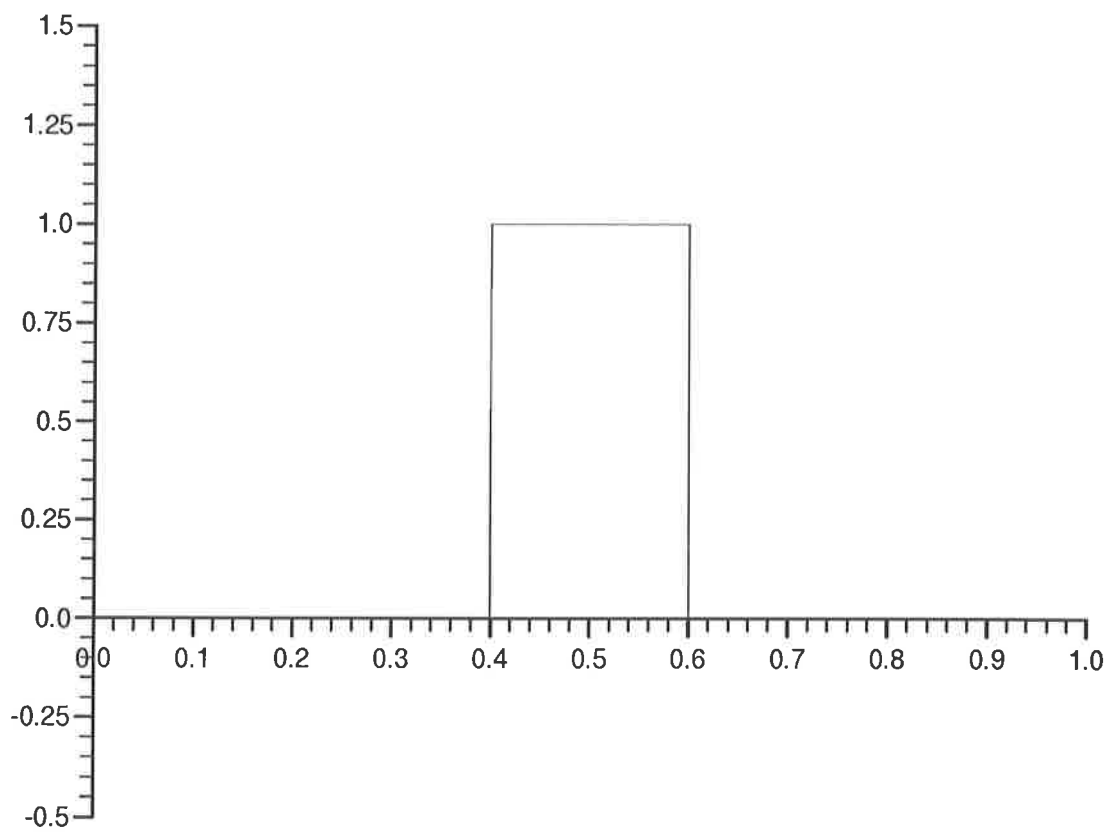


Figure 1: Initial data for advection problem.

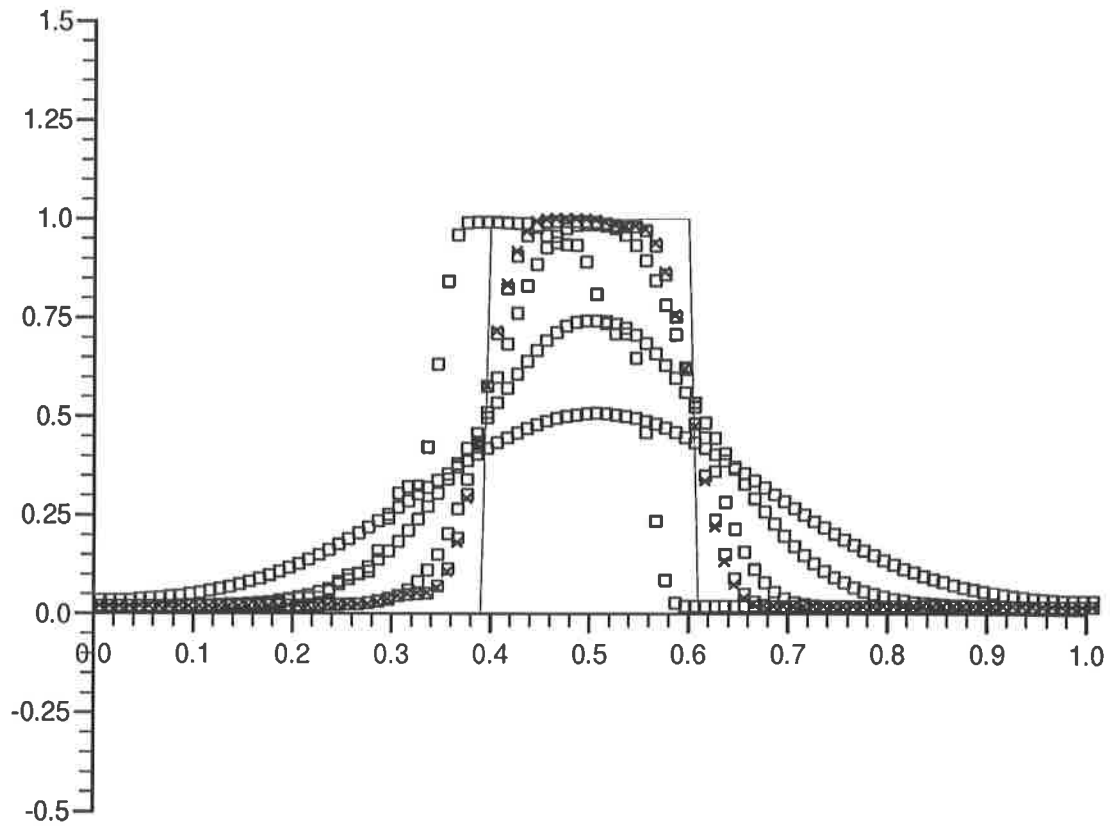


Figure 2: Constant advection after ten rotations. Exact solution—solid line, Monotone 3,4,5,7 (with large phase error) & 8 pt. Gauss-Lobatto—□'s, Monotone exact integration—×. $\Delta x = 1/100$, $\nu = 1/12$.

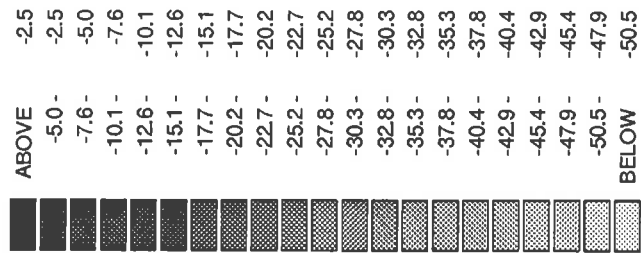
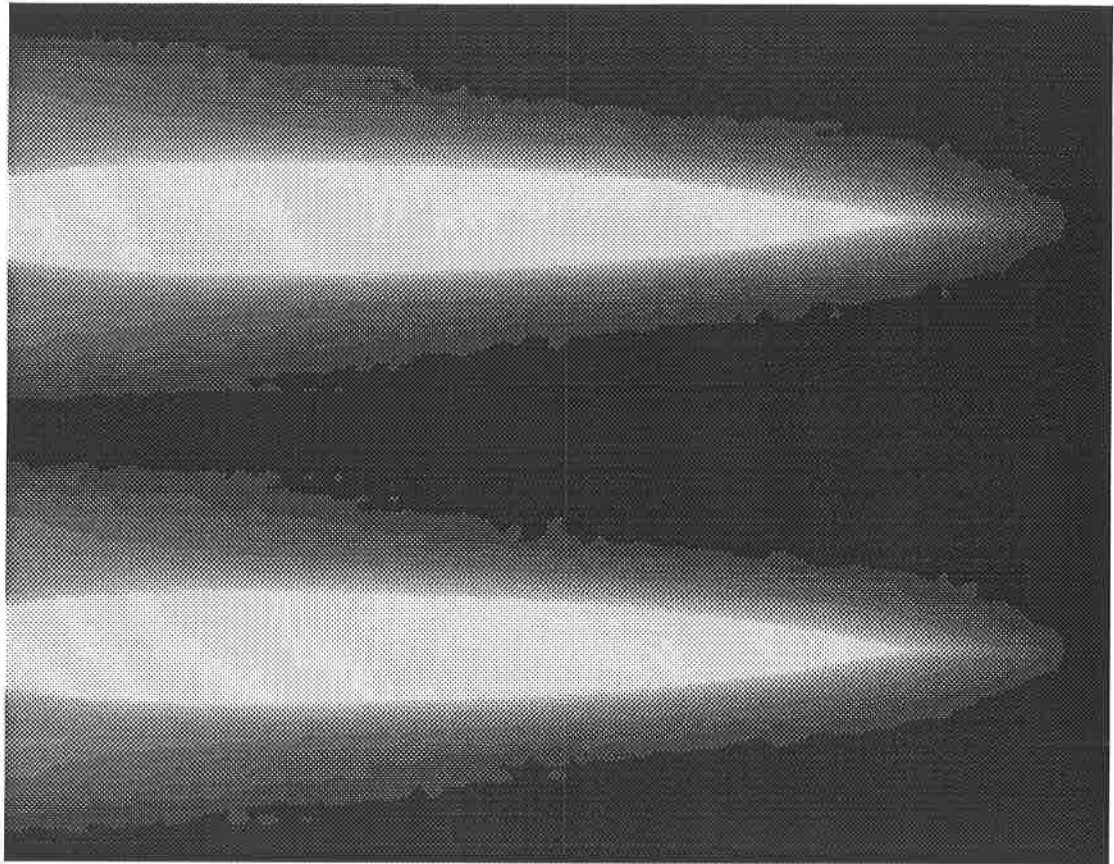


Figure 3: Plot of $(\|A\|_2 - 1) \times 10^6$ for Gauss-Legendre quadrature. Ranges of θ & ν are $[0, 2\pi] \times [0, 0.07]$. $\max(\|A\|_2) = 1$, $\min(\|A\|_2) = 0.999947$.

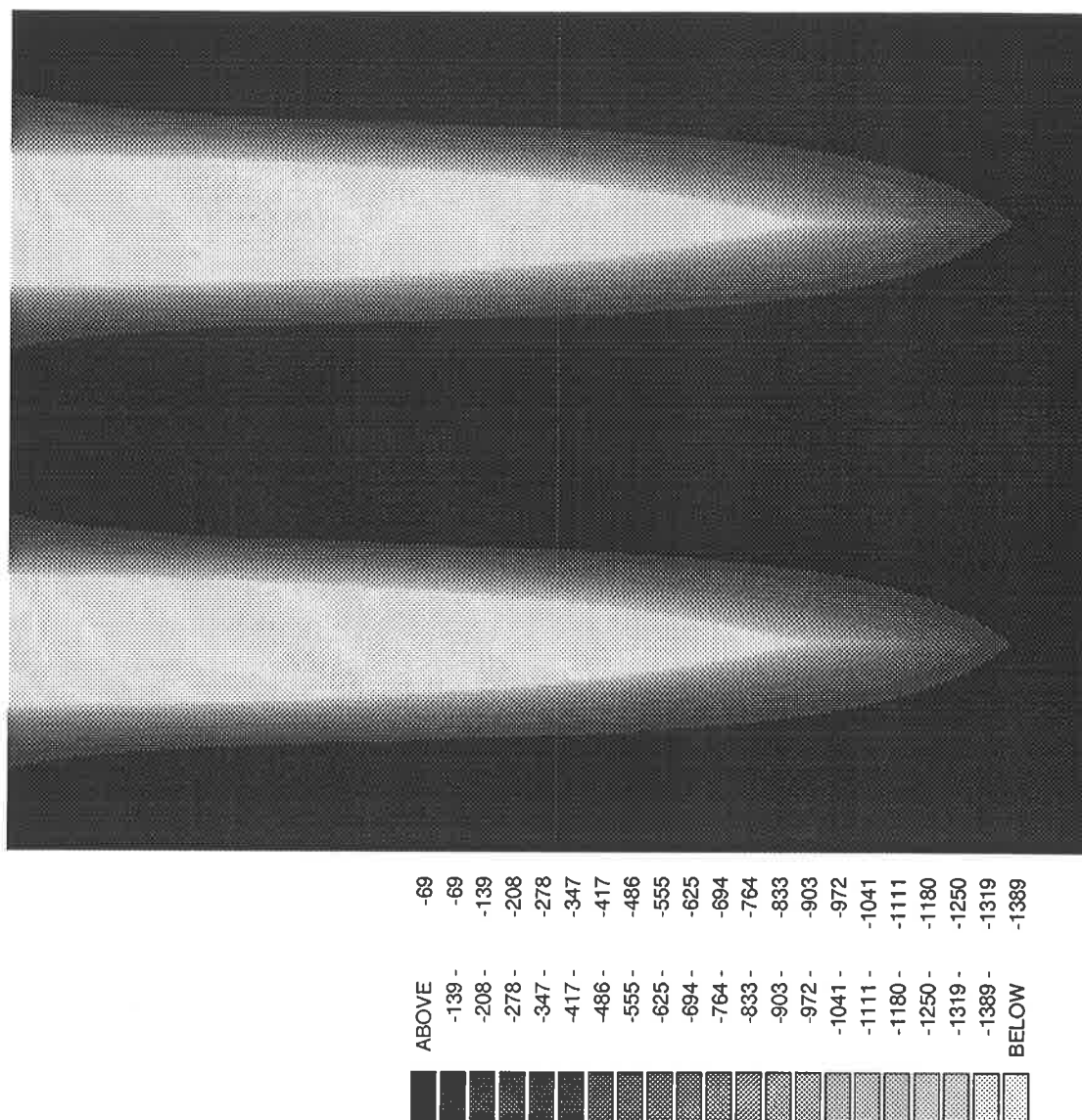


Figure 4: Plot of $(\|A\|_2 - 1) \times 10^6$ for 5 point Gauss-Lobatto quadrature. Range of θ & ν are $[0, 2\pi] \times [0, 0.18]$. $\max(\|A\|_2) = 1$, $\min(\|A\|_2) = 0.998542$.

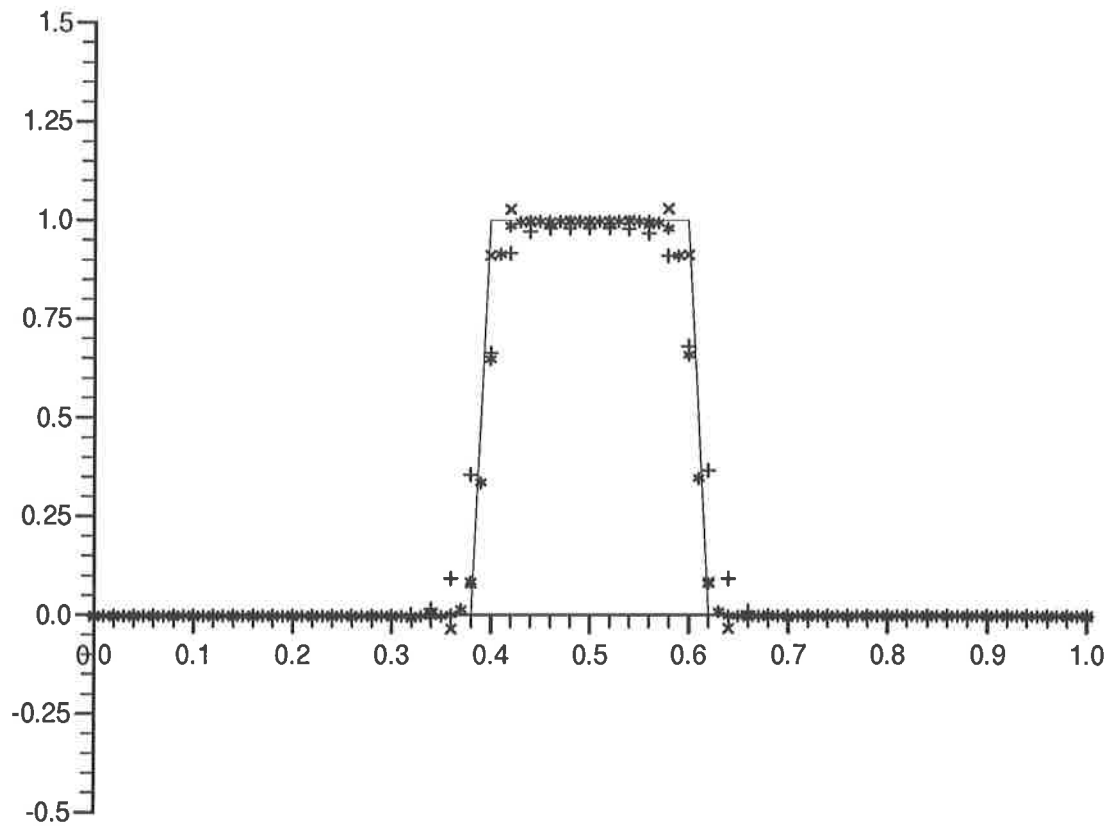


Figure 5: Constant advection after ten rotations. Exact solution—solid line, Superbee ($\Delta x = 1/50$)—+, Superbee ($\Delta x = 1/100$)—*, Lagrange-Galerkin using 5pt. Gauss-Legendre quadrature— \times . $\nu = 5/12$.

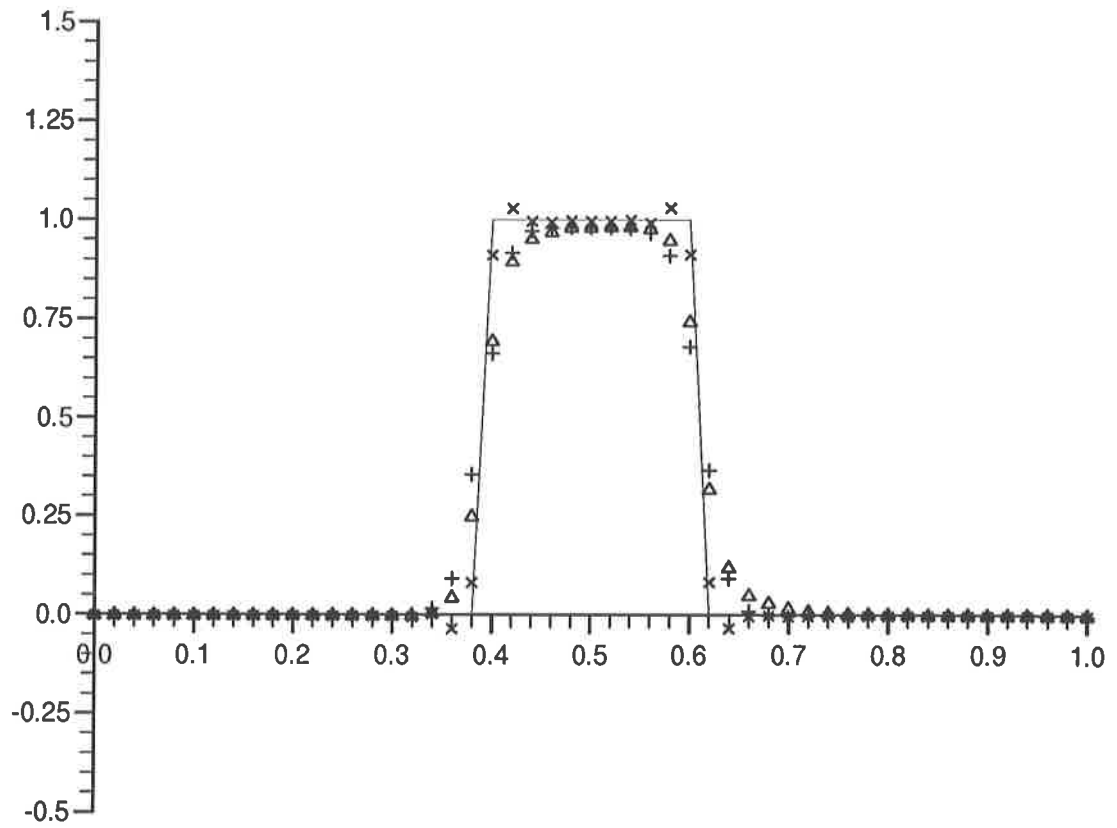


Figure 6: Constant advection after ten rotations. Exact solution—solid line, Superbee — +, Lagrange-Galerkin using 5pt. Gauss-Legendre quadrature— \times , monotone Lagrange-Galerkin using 5pt. Gauss-Legendre — Δ . $\nu = 5/12, \Delta x = 1/50$.

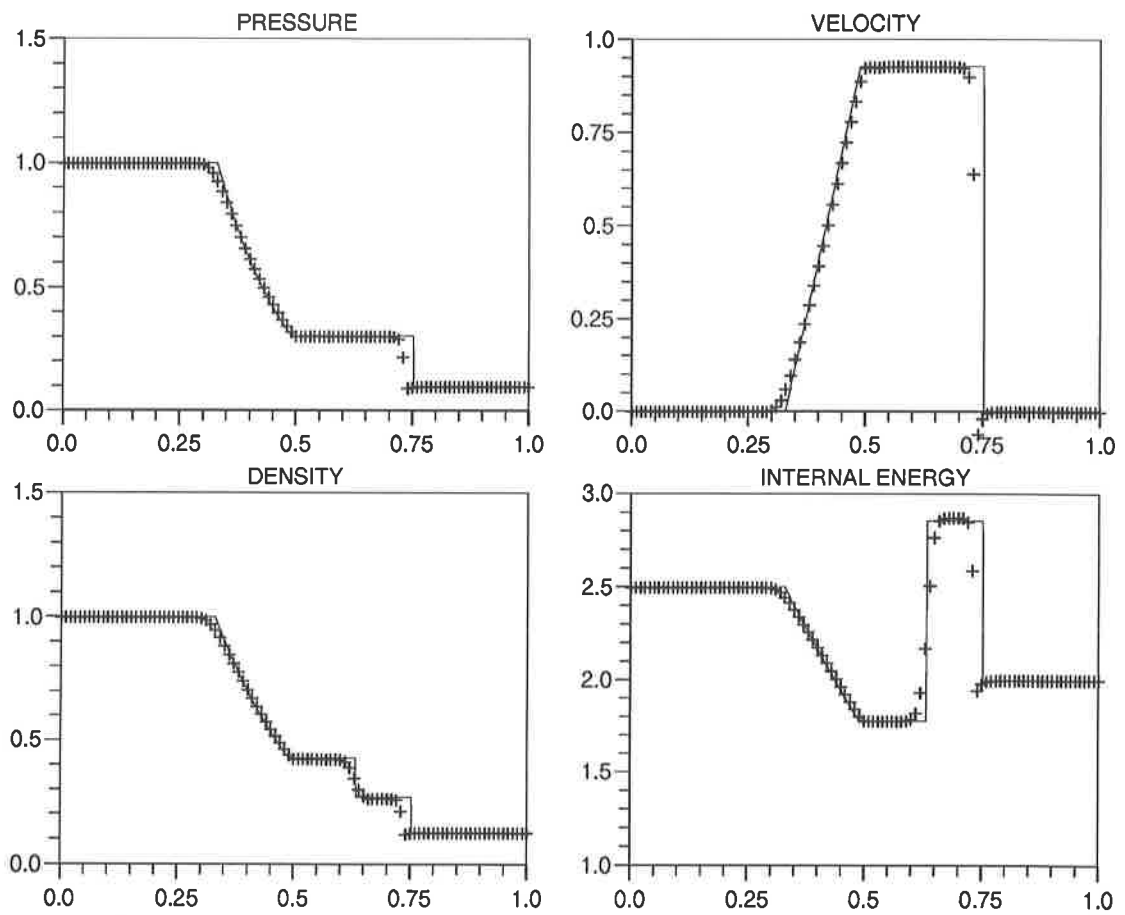


Figure 7: Sod's problem with the Lagrange-Galerkin method evaluated by 8 pt. Gauss-Lobatto quadrature. $\max \nu = 0.22, \Delta x = 1/100$.

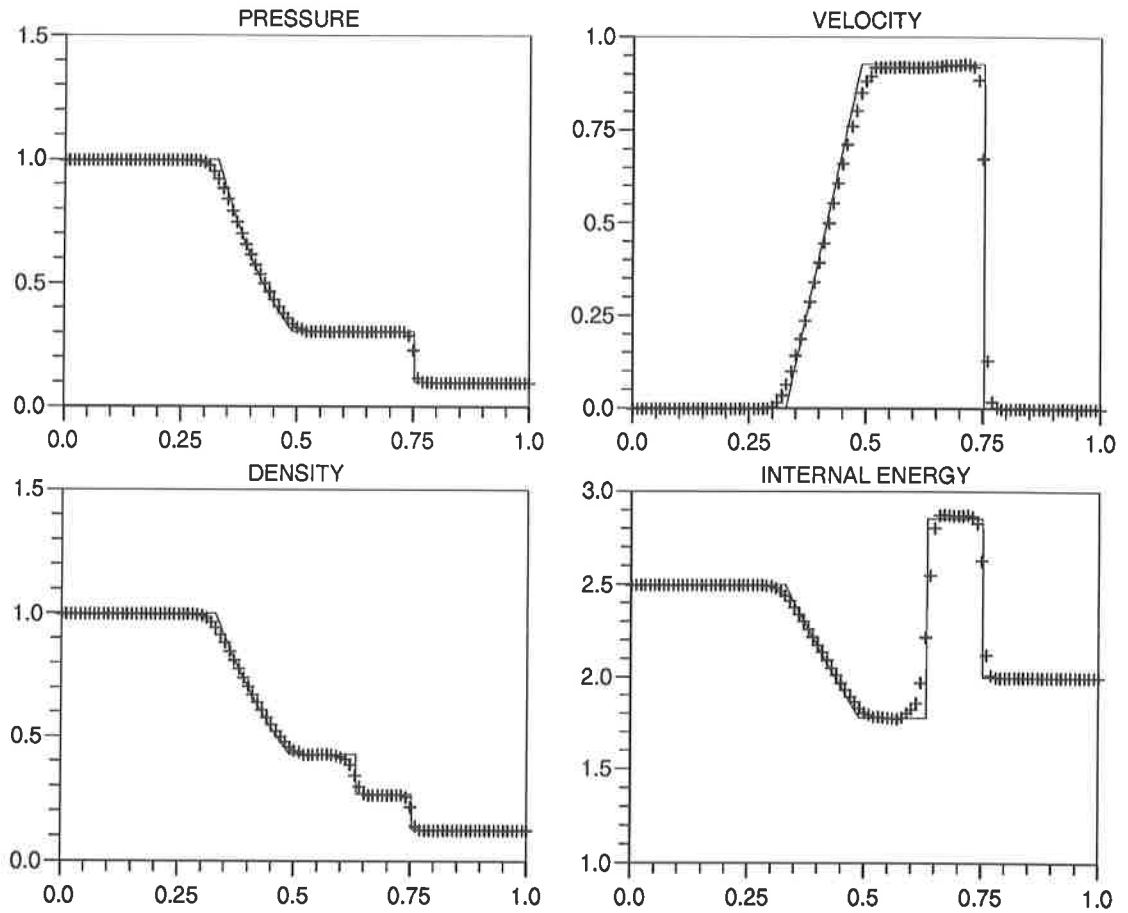


Figure 8: Sod's problem with monotonic Lagrange-Galerkin evaluated by 8 pt. Gauss-Lobatto quadrature. $\max \nu = 0.22, \Delta x = 1/100$.

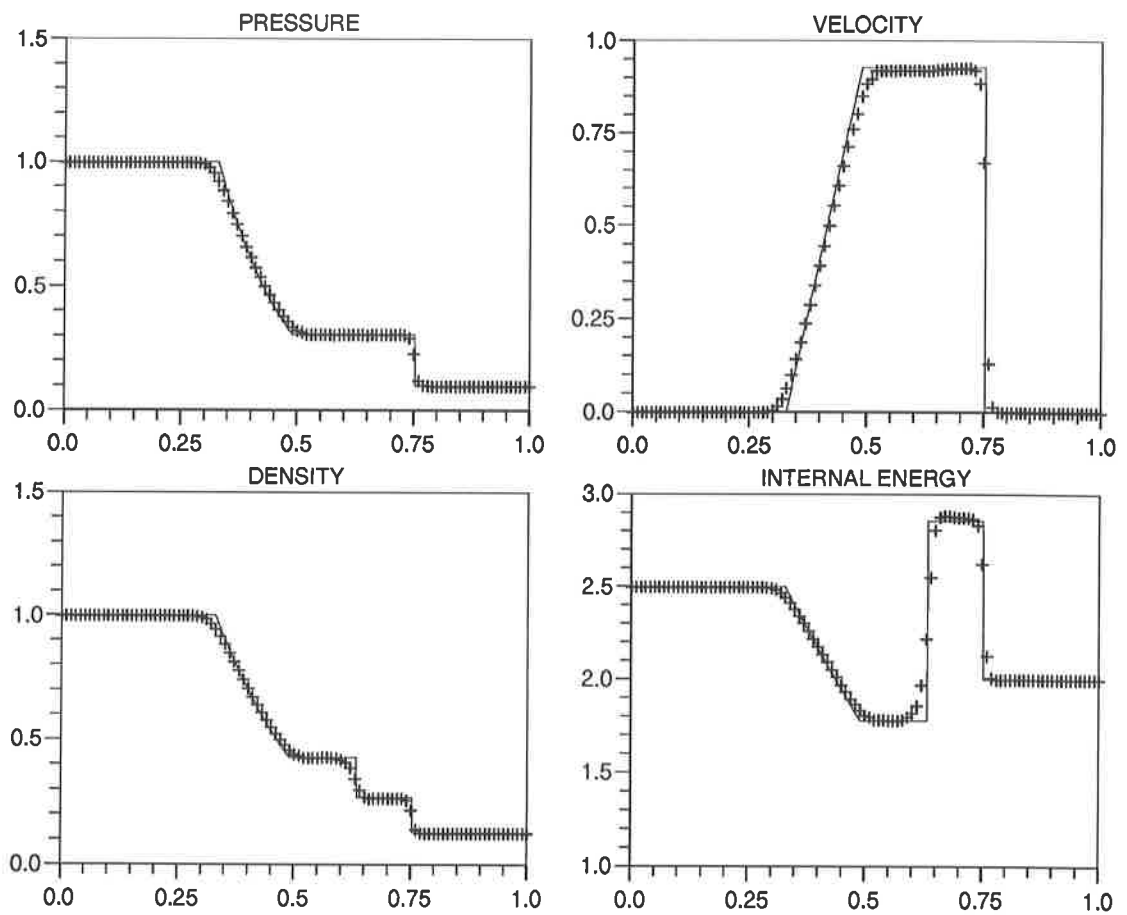


Figure 9: Sod's problem with monotonic Lagrange-Galerkin evaluated by 4 pt. Gauss-Legendre quadrature. $\max \nu = 0.22$, $\Delta x = 1/100$.